Absorber topography dependence of phase edge effects

Aamod Shanker*[a], Martin Sczyrba[b], Brid Connolly[c], Laura Waller[a], Andy Neureuther[a],

[a]Department of Electrical Engineering and Computer Sciences,
253 Cory Hall, University of California, Berkeley, CA 94720-1770;
[b]AMTC, Raehnitzer Allee 9, 01109 Dresden, Germany;
[c]Toppan Photomasks Dresden, Raehnitzer Allee 9, 01109 Dresden, Germany

ABSTRACT

Mask topography contributes to phase at the wafer plane, even for OMOG binary masks currently in use at the 22nm node in deep UV (193nm) lithography. Here, numerical experiments with rigorous FDTD simulation are used to study the impact of mask 3D effects on aerial imaging, by varying the height of the absorber stack and its sidewall angle. Using a thin mask boundary layer model to fit to rigorous simulations it is seen that increasing the absorber thickness, and hence the phase through the middle of a feature (*bulk phase*) monotonically changes the wafer-plane phase. Absorber height also influences best focus, revealed by an up/down shift in the Bossung plot (linewidth vs. defocus). Bossung plot tilt, however, responsible for process window variability at the wafer, is insensitive to changes in the absorber height (and hence also the *bulk phase*). It is seen to depend instead on EM edge diffraction from the thick mask edge (*edge phase*), but stays constant for variations in mask thickness within a 10% range. Both *bulk phase* and *edge phase* are also independent of sidewall angle fluctuation, which is seen to linearly affect the CD at the wafer, but does not alter wafer phase or the defocus process window. Notably, as mask topography varies, the effect of *edge phase* can be replicated by a thin mask model with 8nm wide boundary layers, irrespective of absorber height or sidewall angle. The conclusions are validated with measurements on phase shifting masks having different topographic parameters, confirming the strong dependence of phase variations at the wafer on *bulk phase* of the mask absorber.

1. INTRODUCTION

Thick mask effects cause phase variations across features in the aerial image at the wafer plane of a lithographic stepper. This wafer-plane phase will introduce asymmetry in the intensity through-focus, causing shrinkage of the process window (Fig 1). With the advent of more absorbing materials, industry has switched to thinner binary masks from the higher contrast phase shifting masks in an attempt to mitigate undesirable phase due to mask thickness. The attenuating OMOG (Opaque MoSi on Silica) masks designed by Shin-Etsu, for instance, use a high-k material to achieve large extinction with a thinner absorber.[1] However, phase effects at the wafer still persist for OMOG masks, causing defocused intensity to deviate from the symmetrical behavior expected for an ideal binary mask (Fig 1).

Lithographic processes are often evaluated with focus exposure matrices (FEMs), where the critical dimension (CD) of a feature is plotted against defocus for various exposure levels (or conversely for various resist thresholds). These "Bossung" plots are a good indicator of process window with respect to focal budget and exposure latitude for a given CD tolerance.[2] Since the presence of phase at the mask causes intensity to be asymmetric through-focus, it causes the Bossung plot to tilt. The Bossung tilt will lead to a smaller focal budget, and can thus be used as a measure of the loss in process window due to topographic phase effects.

In previous work,[3] using experimental images of an OMOG absorber taken with AIMS^{TM} (Aerial Imaging Measurement System[4]), the wafer phase across a feature was obtained from a through-focus intensity stack by solving the Transport of Intensity Equation (TIE) .[5,6] It was observed that significant phase modulation does exist across the absorber, especially when illumination polarization is perpendicular to the feature edge (TM), seen in Fig. 2. This undesired phase is a consequence of the mask topography, and must be modeled in order

* Correspondence
Aamod Shanker: aamod@berkeley.edu

Photomask Technology 2015, edited by Naoya Hayashi, Bryan S. Kasprowicz, Proc. of SPIE
Vol. 9635, 96350G · © 2015 SPIE · CCC code: 0277-786X/15/$18 · doi: 10.1117/12.2197861

Downloaded From: http://proceedings.spiedigitallibrary.org/ on 11/08/2016 Terms of Use: http://spiedigitallibrary.org/ss/termsofuse.aspx

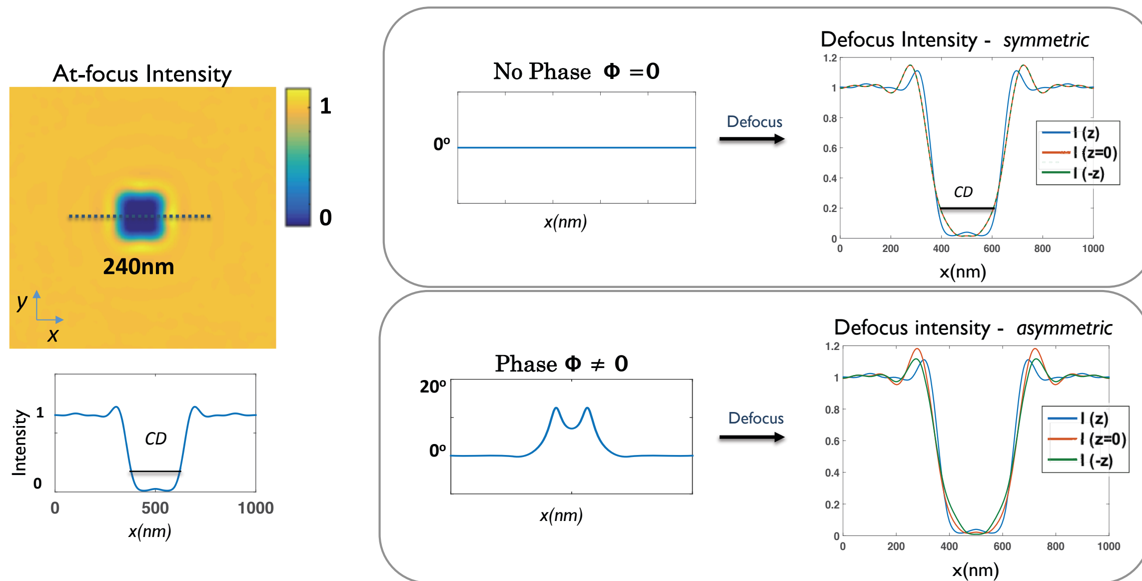

Figure 1. Intensity variations through-focus depend on both intensity and phase at the mask. For an ideal binary mask with no phase effects (simulation), positive and negative defocus produce the same intensity curves; hence, defocus is symmetric through-focus (top right). A real OMOG mask has phase modulation across the feature at the wafer plane, which causes symmetry-breaking such that intensity is different on either side of focus (bottom right).

to be mitigated. A common approach to include phase introduced by mask 3D topography in thin mask models is to decorate feature edges with complex-valued boundary layers[7–9] that represent diffraction effects. Here we will use a similar boundary layer framework to identify phase due to topographical factors on the mask.

It has also been demonstrated that mask topography impact on aerial imaging can indeed be mitigated with absorber design; studies on mask thickness dependence of best focus[10,11] show that a thinner absorber causes smaller phase effects at the wafer, reduces shifts in best focus, and lessens linewidth variation through-focus. In what way exactly the wafer phase and Bossung plot relate to mask phase, however, still needs clarification. More specifically, what is the contribution of phase through the large area of the absorber stack (*bulk phase*) vs. contribution from diffraction at the sidewall (*edge phase*), and how do each influence wafer phase? Additionally, how does the wafer phase influence aerial image behavior through-focus? Even though the qualitative dependence of defocus behavior on wafer phase has been observed previously,[8,12] an explicit analytic relationship between linewidth variation through-focus and wafer phase, derived here, is essential to relate phase effects to the lithographic process window.

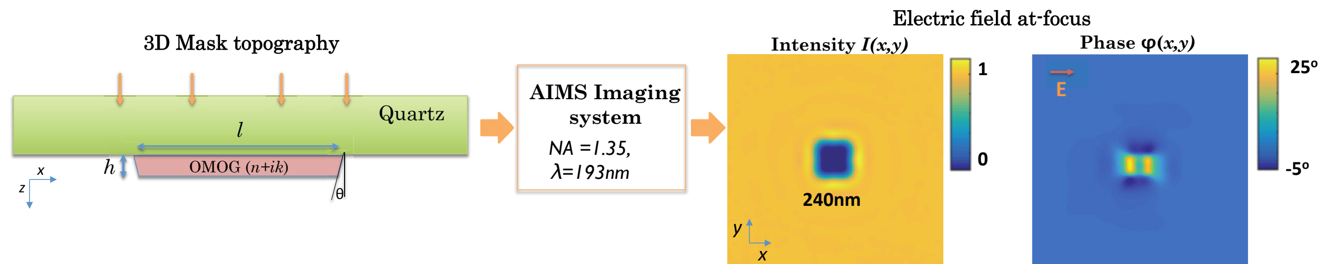

Figure 2. Topography of the absorber stack causes polarization-dependent phase modulation across the feature at the aerial image, as seen in this measurement of a 240nm absorbing OMOG contact, imaged with an aerial imaging (AIMS) tool. The phase is recovered by measuring a stack of through-focus intensity measurements and solving for phase at-focus.

Downloaded From: http://proceedings.spiedigitallibrary.org/ on 11/08/2016 Terms of Use: http://spiedigitallibrary.org/ss/termsofuse.aspx

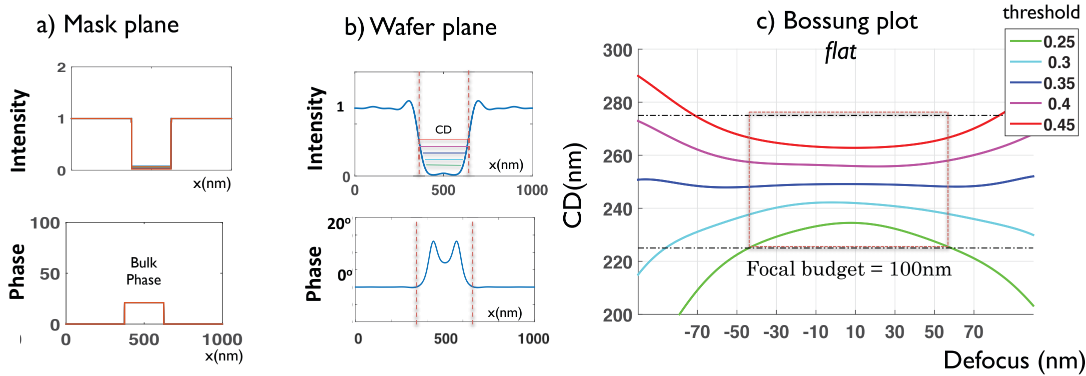

Figure 3. a) Thin mask simulations with a constant *bulk phase* across the absorber. b) Even though bulk phase modulates the wafer-plane phase, phase gradients still fall to zero at the position where CD is defined on the aerial image (red dots). c) As a result, Bossung plots are symmetric about focus, allowing a wide focal budget.

This work analyzes mask topography effects with rigorous electromagnetic (EMF) simulations of the thick mask to investigate its influence on wafer phase and Bossung behavior. Studies are performed for TM polarization for a 240nm isolated feature (except in Sec. 6), using a threshold-based resist model to define CD in the aerial image with partial coherence of $\sigma = 0.3$. First, a small-defocus linearization is developed, which algebraically relates the wafer phase to Bossung tilt, and hence to process window. Next, as the topography varies, the contribution of *edge phase* and *bulk phase* at the mask to the phase at wafer are identified using comparisons with a thin mask model, and their individual impact on the Bossung plot is studied. Finally, our conclusions are verified with aerial image experiments, demonstrating the dependence of wafer phase on the mask parameters as discovered in simulations.

The layout is as follows: Sections 2 and 3 explore the relationship between wafer phase and Bossung tilt, arriving at an algebraic expression connecting the two. Sections 4-6 study the impact of absorber height, sidewall angle and feature size on wafer phase and Bossung tilt. Subsequently, experiments on ATT-PSM masks are used to confirm predicted trends (Sec. 7).

2. BOSSUNG TILT DEPENDENCE ON WAFER PHASE

To identify the contributions of the *edge phase* and *bulk phase* at the wafer, their individual impact on the Bossung plots and wafer-plane phase is studied. First, the relationship between Bossung plots (CD vs defocus) and wafer phase is demonstrated using through-focus aerial image simulations of a thin mask.

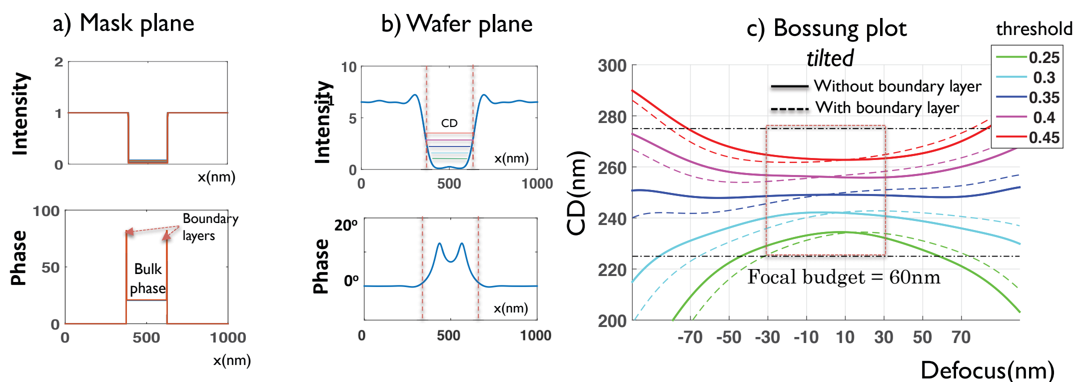

Figure 4. a) Boundary layers are added in the thin mask model, along with bulk phase. b) As a result phase gradients are no longer zero at the feature edge at the wafer plane. c) This causes the Bossung plots defined at various thresholds to tilt, forcing the focal budget centered about best-focus to shrink by about 40nm compared to Fig. 3c.

Downloaded From: http://proceedings.spiedigitallibrary.org/ on 11/08/2016 Terms of Use: http://spiedigitallibrary.org/ss/termsofuse.aspx

Figure 3 simulates an absorbing contact in the ideal thin mask case - with a constant *bulk phase* across the absorber, but no boundary layers to model the *edge phase*. The Bossung plot is shown for five different thresholds, corresponding to decreasing exposure from green to red. Even though the wafer-plane phase shows up to 15° modulation across the feature, it is interesting to see that the Bossung plot is flat (i.e. CD is symmetric about defocus). Intensity is thus symmetric about focus at the feature edges, but not necessarily at other positions on the feature. As explained later in Sec. 3, Bossung tilt depends on wafer phase gradients at the position where the CD is defined (red dashed lines in Fig. 3b) ; in this case the phase gradient falls to zero at the edge, thus yielding a flat Bossung. The process window impact can further be quantified in terms of focal budget - for a CD tolerance of 10%, the focal budget is the smallest focus range that can contain the CD within tolerance for given range of exposure - in this case the Bossung is flat, and hence the focal budget is a healthy 100nm (Rayleigh depth of focus being about 140nm for given $\lambda = 193nm$, NA = 1.4).

Now we introduce complex-valued additive boundary layers at the feature edge ($1\angle 90°$, 8nm wide) that represent *edge phase* at the mask. This causes the wafer phase across the feature to spread, such that phase gradients are no longer zero at the edge (Fig. 4b). This reflects as a tilt in the Bossung plot, shown as dotted curves in Fig. 4c. The tilt compromises the focal range that permits the CD to stay within tolerance for the given exposure range. In this example, the focal budget is narrowed to 60nm (from 100nm for a flat Bossung), shrinking the process window significantly. Note that the best focus (the peaks of the Bossung plots) may change for a tilted Bossung, even if it shifts up or down with no additional tilt, for instance on changing the absorber height as we shall see later. However, this is not a fundamental loss in process window, since a shift of the Bossung plot can be compensated by redefining zero focus and nominal CD.

3. CD-TIE : QUANTIFYING BOSSUNG TILT VS. WAFER PHASE

Clearly, Bossung tilt is directly related to wafer phase - the dependence is now quantified for the region near focus, based on the Transport of Intensity Equation (TIE). The TIE expresses the changes of intensity through-focus (z) in terms of the phase (ϕ) derivative in the lateral dimensions (x, y) at the focal plane,

$$\frac{dI}{dz} = -\frac{\lambda}{2\pi}\nabla \cdot I\nabla\phi, \tag{1}$$

where $\nabla = \frac{d}{dx}\hat{x} + \frac{d}{dy}\hat{y}$ is the two-dimensional gradient operator. This linear formulation relies on a paraxial approximation and small defocus assumption. Originally, the TIE was derived to solve for phase from intensity images through-focus (which is the basis of our experimental phase retrieval methods). Here, we use the same equation to instead derive a quantitative relationship between phase effects and Bossung tilt, in terms of CD.

The Bossung tilt (CD vs. defocus) near focus can be related to the phase of the electric field at-focus starting from the 1D TIE, since CD is defined for one dimension at a time,

$$\frac{dI}{dz} = -\frac{\lambda}{2\pi}\frac{d}{dx} \cdot I\frac{d\phi}{dx}. \tag{2}$$

Expanding the derivative on the right side of Eq. 2, and multiplying the left by dx/dx, we get,

$$\frac{dI}{dx}\frac{dx}{dz} = -\frac{\lambda}{2\pi}\left[\frac{dI}{dx} \cdot \frac{d\phi}{dx} - I\frac{d^2\phi}{dx^2}\right]. \tag{3}$$

Since a change in the x position of the aerial image (at resist threshold) with defocus z corresponds to a change in the critical dimension (CD), then for a laterally symmetric feature (which introduces a factor of 2) one can equate $2dx/dz = dCD/dz$. In this way, Eq. 3 can be re-written as

$$\frac{dCD}{dz} = -\frac{\lambda}{\pi}\left[\frac{d\phi}{dx} - \frac{I}{dI/dx}\frac{d^2\phi}{dx^2}\right], \tag{4}$$

which we call the CD-TIE. The CD-TIE relates the Bossung tilt around focus (dCD/dz) to the phase (ϕ) and intensity (I) derivatives where the resist threshold meets the aerial image (dotted lines in Fig. 4b). Hence,

Downloaded From: http://proceedings.spiedigitallibrary.org/ on 11/08/2016 Terms of Use: http://spiedigitallibrary.org/ss/termsofuse.aspx

the Bossung tilt depends strongly on the first derivative of phase at the feature edge, but also on the second derivative of the phase weighted by the inverse Normalized Image Log Slope, NILS $= (dI/dx)/I$. Typically, the second derivative of the phase is much smaller than the first term, and hence is negligible for a high NILS. In the situation of Fig. 4, for instance, $d\phi/dx = 7.7 \times 10^{-4}m^{-1}$, while $\frac{1}{NILS}d^2\phi/dx^2 = 2.3 \times 10^{-8}m^{-1}$, so the second term is negligible. The first derivative of phase at the feature edge is therefore the main factor causing the Bossung to tilt by 0.04nm/nm in CD per defocus units.

An intuition for the effect of phase derivatives in the CD-TIE can be obtained by considering Huygen's principle, which states that light propagates normal to phase fronts. The first term on the right side of Eq. 4, containing the first derivative of phase, models intensity steering by the local slopes of phase front with propagation, while the second term represents focusing from the local curvatures in the phase front.[13] The left-hand side is a finite difference of the CD on either side of focus. The end result is a quantification of how phase derivatives at the feature edge determine Bossung tilt, which in turn impacts the process window.

4. IMPACT OF ABSORBER HEIGHT ON AERIAL IMAGING

How do the phase at the wafer and Bossung plot respond to the fluctuations in mask topography? We start with an absorber modeled as a trapezoid (n =1.23, k =1.45), with topography variations being approximated by changes in absorber height and sidewall angle. This section studies the dependence of aerial imaging performance on absorber height variations, with the analysis for sidewall angle in the next section.

A rigorous EMF solver (Panoramic EM Suite[14]) is used to investigate the variation of aerial imaging performance with up to 10% fluctuations in the height of a simulated OMOG absorber, as shown in Fig. 2. The simulations use DUV light with wavelength λ = 193nm. The imaging is with a monopole source (incoherence parameter σ = 0.3) and numerical aperture NA=1.4. The imaging system simulates low-pass filtering by the NA and summing over each point of the partially coherent illumination to obtain wafer-plane fields.

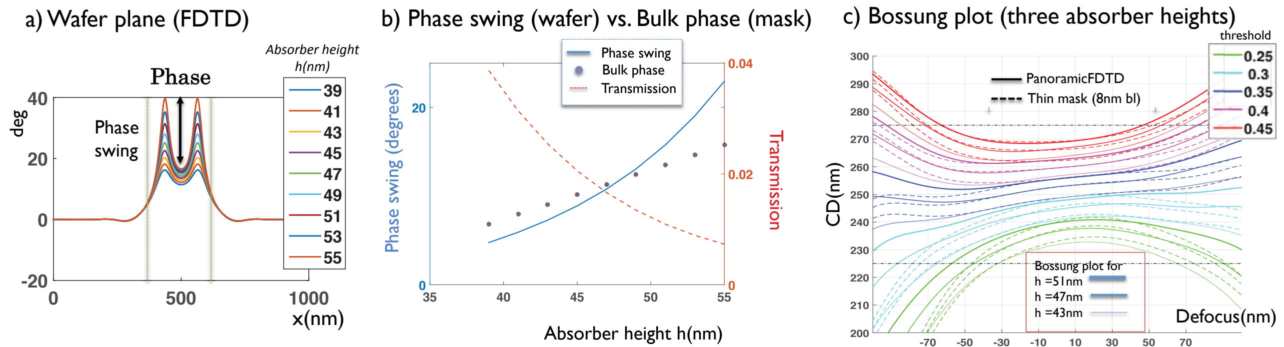

Figure 5. Variation in wafer-plane phase with 10% variation in absorber height. a) The wafer-plane phase swing increases with absorber height, although gradients at the feature edge stay about the same. b) The phase swing closely follows the calculated *bulk phase* with increasing absorber height, while transmission drops exponentially for given material. c) The Bossung plot shifts upward for increasing absorber height, with no change in the tilt (solid lines). The thin mask Bossung plot (dotted lines) needs to include the changing *bulk phase* and a constant *edge phase* to get a good fit.

Changing the absorber height modulates the *bulk phase* linearly, since phase through the large area absorber ($\frac{2\pi}{\lambda}h \times n$) depends linearly on absorber height h (dots in Fig. 5b). The phase at the aerial image has taller peaks as the absorber gets thicker (Fig. 5a), the phase swing following the increasing trend of *bulk phase* through the absorber. The sensitivity of the phase to absorber height is about 1°/nm - larger than the drop in absorption (0.13%/nm). Hence, phase at the wafer could be used as a sensitive metric for measuring absorber thickness.

Furthermore, changing absorber height shifts the Bossung plot upward, *without affecting its tilt* (Fig. 5c), since the phase gradient at the feature edge is about the same for all heights. This will also cause best focus (Bossung maxima) to walk linearly with absorber height. This is not a loss in the fundamental process window however, which can be regained simply by redefining optimal focus and nominal CD. As we saw in Sec. 2, the tilt is caused by edge diffraction at the mask sidewall (*edge phase*), which must hence also be insensitive to absorber height. Next we quantify the exact contribution using a thin mask model to fit to the FDTD wafer phase.

Downloaded From: http://proceedings.spiedigitallibrary.org/ on 11/08/2016 Terms of Use: http://spiedigitallibrary.org/ss/termsofuse.aspx

4.1 Thin mask modeling : *bulk phase* vs *edge phase* contributions of thick absorber

While the EMF simulations, followed by aerial imaging generates the net electric fields at the wafer plane, it is not trivial to isolate contributions from the bulk vs edge of the absorber, since the mask near-field has been low-pass filtered by the imaging system. A thin mask approximation that treats the phase in the near field as a sum of *bulk phase* and *edge phase* will give insight into the amount of edge diffraction in play at the mask.

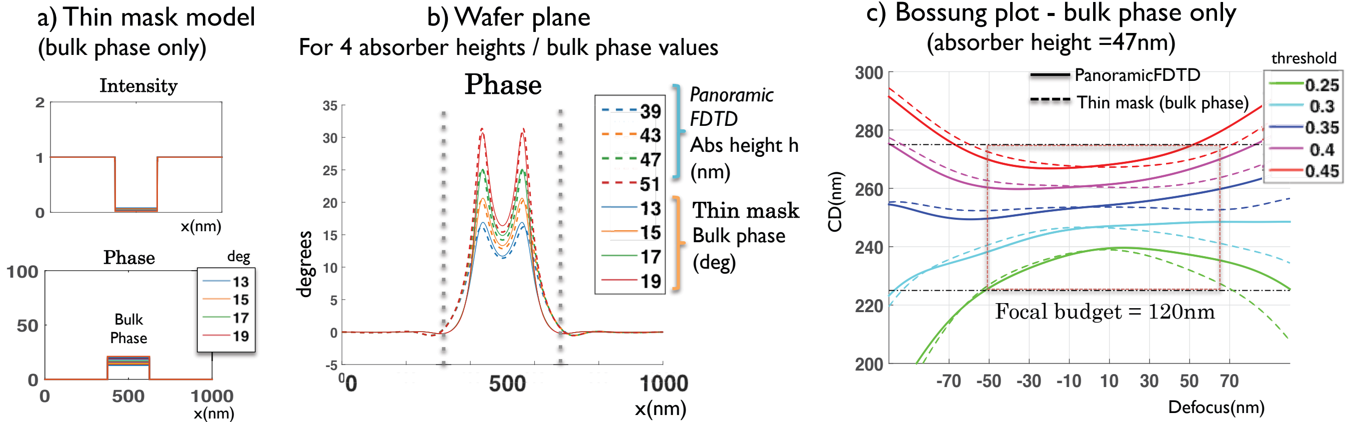

Figure 6. Thin mask simulations without *edge phase* modeled do not fit well to wafer phase calculated with rigorous simulations. a) The thin-mask *bulk phase* is varied linearly as the absorber gets thicker, ignoring edge phase effects. b) The wafer-plane phase matches the phase swing of rigorous simulations, but does not match at the feature edges (dotted lines). c) The Bossung tilt is not captured by the thin mask model (dashed curves) since *edge phase* has not been modeled.

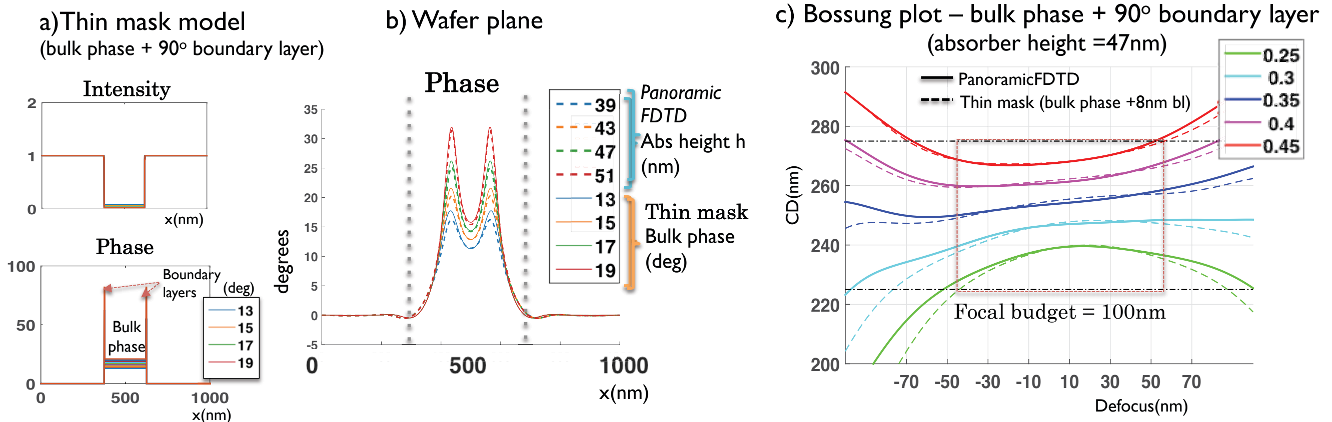

Figure 7. Thin mask simulations with both *bulk phase* and *edge phase* effects fit well to wafer-plane phase from rigorous simulations. a) Thin mask model with 8nm wide, imaginary-valued (90°) boundary layers added at the feature edge to represent *edge phase*. b) The phase profiles are now well replicated when compared to the rigorous result, accurately capturing the phase gradients at the feature edge. c) Bossung tilt depends on phase gradient at edges, and is now matched.

Bulk phase is first modeled in the thin mask as a constant phase across the feature (Fig. 6a). After imaging, the phase at the wafer is compared to the EMF result in Fig. 6b. While the peak phase swing can be matched to rigorous simulation by changing the *bulk phase* linearly with absorber height, notice that at the feature boundary, the widths of the phase profiles do not match. In fact, there exists no value of *bulk phase* on the thin mask that can provide a good match. The addition of phase at the edges is necessary for a good fit. Additionally the Bossung tilt seen in rigorous simulation is not replicated by this thin mask when imaged to the wafer (Fig. 6c), unless *edge phase* is included in the model.

Next, we show that it is possible to obtain a good fit to EMF simulations if both *bulk phase* and *edge phase* are included on the thin mask. The *edge phase* is modeled as thin mask boundary layers at the edge of the

Downloaded From: http://proceedings.spiedigitallibrary.org/ on 11/08/2016 Terms of Use: http://spiedigitallibrary.org/ss/termsofuse.aspx

absorbing feature. Figure 7 shows the same fitting as Fig. 6, but with an 8nm phase, imaginary-valued ($1\angle 90°$) boundary layer added to the edges of the feature at the thin mask. The boundary layer is of quadrature phase (90°) since both 0° and 180° correspond to a real valued mask, with no Bossung tilt. Irrespective of absorber height, the same width and value of the additive boundary layer fits the phase profile, widening the thin mask wafer-plane phase to achieve an overlap with the rigorous result (Fig. 7b). Moreover, the same boundary layer is able to replicate the Bossung tilt as well (Fig. 7c), since the wafer phase gradients are now matched - in this example the tilt leads to a loss of about 20nm in the focal budget. Hence the *edge phase* model can be used to accurately fit to rigorous simulations, whereas the *bulk phase* only model cannot - we infer that phase due to thick mask edge effects (*edge phase*) is critical for modeling mask topography impact on process window.

Two key observations should be noted. First, the boundary layer, and hence edge diffraction, are independent of absorber height within the 10% range simulated here. This explains why the Bossung plot tilt is independent of absorber height fluctuations in EMF simulation (thick lines in Fig. 5c) , and is matched with a constant boundary layer for each case (dotted lines in Fig. 5c) . Second, the boundary layers representing edge diffraction influences the width of the wafer phase profile at feature edges, *but not its peak swing*. It is the width of the phase bumps that matters for determining the process window, since they determine the phase gradients ($d\phi/dx$) at the feature edge, which affect the Bossung tilt (dCD/dz), as was shown by the CD-TIE (Eq. 4).

These findings can be further related to previous investigations by Finders[10] and Erdmann et. al.,[15] which showed that the phase of the 0th order in the pupil affects the best focus at the aerial image for dense line-space patterns. Although we are looking only at an isolated contact here, the phase of the 0th order, if thought of as the average phase across the near field, would nevertheless correspond one-to-one with the *bulk phase* through the contact. Larger *bulk phase*, which consequently means smaller absorption, will shift the CD up, and (if there is a Bossung tilt) will also cause best focus to walk for various thresholds. Another interesting conclusion is that in the hypothetical absence of edge diffraction, the Bossungs will not be tilted, and despite the CD curves moving up/down, best-focus would remain unaffected.

5. IMPACT OF ABSORBER SIDEWALL ANGLE ON AERIAL IMAGING

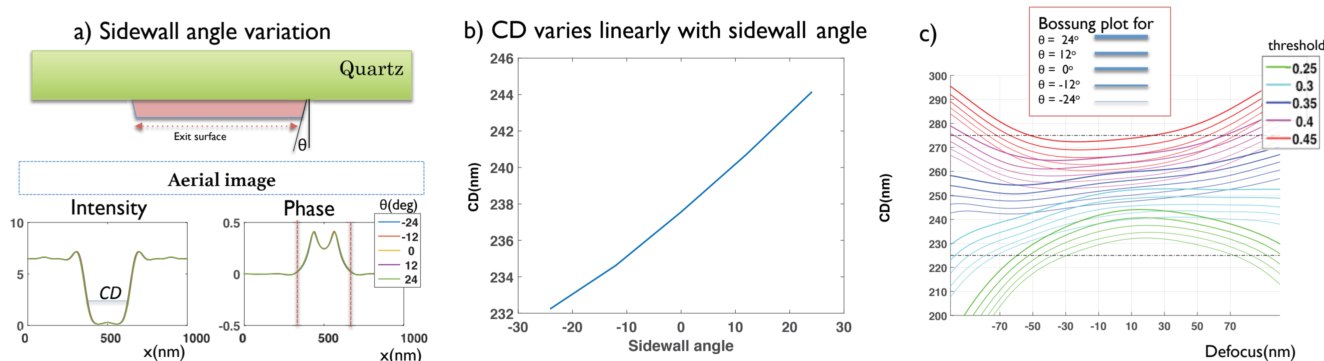

Figure 8. Sidewall angle changes the CD at the wafer, but leaves the phase and Bossung tilt unaffected. a) Sidewall angle change causes no variation in phase (overlapping curves). b) The CD depends on the size of the exit surface of the absorber, and hence gives a linear increase with sidewall angle. c) The Bossungs shift up due to the increased CD with increasing sidewall angle, which may affect Bossung maxima (best-focus) but not Bossung tilt (or process window).

The next aspect of mask topography studied is the sidewall angle. The sidewall angle is varied by modifying the width of the exit surface of the absorber stack (bottom surface in Fig. 8a), over a range representing sidewall angles from $-25°$ to $25°$. The aerial image is then generated by low-pass filtering the near-fields output from the EMF simulator, as before. Results show that the wafer phase is unaffected by sidewall angle changes, with the phase curves in Fig. 8a overlapping.

The CD defined at a fixed threshold (0.35 here, chosen at the isofocal point), however, varies linearly with sidewall angle (Fig. 8b), indicating that the CD at the aerial image is a direct outcome of the width of the

Downloaded From: http://proceedings.spiedigitallibrary.org/ on 11/08/2016 Terms of Use: http://spiedigitallibrary.org/ss/termsofuse.aspx

exit surface of the absorber stack. The Bossung plot of Fig. 8c shows a simple shift up as the sidewall goes from over-cut to undercut, a similar behavior to the Bossung shift with absorber height. This is a result of the CD increasing linearly with sidewall angle (similar to CD vs. absorber height, which also gives a linear relationship for a given threshold). However, since the wafer phase is unaffected, the thin mask model to account for sidewall angle needs only the absorption edge to be shifted on the mask in order to adjust the hole size and hence modulate the CD accordingly. The boundary layers (8nm @ $1\angle 90°$) serving to model the *edge phase*, as well as the *bulk phase*, stay constant in the thin mask. Hence, the sidewall angle, although changing the position of the feature edge, does not affect the wafer phase, Bossung tilt, or process window for an isolated feature.

6. IMPACT OF FEATURE SIZE ON AERIAL IMAGING

It is natural to ask: does the constancy of edge diffraction (*edge phase*) and the linear dependence of *bulk phase* on absorber height hold for a smaller feature size? We show here that it does. Figure 9 shows simulations with a smaller, resolution-limited feature (105nm contact, $\lambda = 193nm$, NA =1.4) than in previous plots. We again use a boundary layer model with 8nm imaginary-valued phase edges, which is able to successfully match the Bossung curve tilt for a given absorber height. This demonstration implies that edge diffraction is also independent of feature size, as predicted. Note that the Bossung tilt for this smaller feature is a smaller fraction of the Bossung curvature, so becomes less noticeable than that for the larger feature studied earlier.

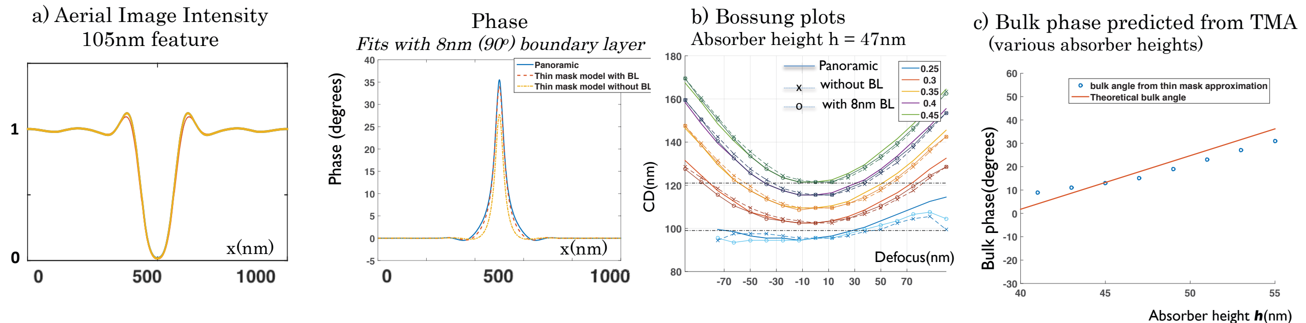

Figure 9. *Edge phase* is invariant with feature size and absorber height, although *bulk phase* still varies linearly with absorber height when looking at a smaller feature. For the smaller feature, the same boundary layer model is able to predict a) the phase at the wafer plane and b) the Bossung tilt for a given absorber height. c) The *bulk phase* needed in the thin mask model to fit to rigorous simulation matches the theoretical bulk phase calculated from the absorber height.

The *bulk phase* in the thin mask model that is required for achieving a good fit with the wafer phase (plotted in Fig. 9c) for different absorber heights shows a good agreement with the *bulk phase* calculated from the optical path for a single pass through the absorber ($\frac{2\pi}{\lambda}n \times h$). Hence, the invariance of edge diffraction, as well as the linear dependence of phase swing on *bulk phase*, holds for features at least down to the resolution limit. This statement may break down if illumination differs from the monopole used in the current study. Off-axis illumination will change the effective phase edge effects at the wafer plane, since each source point passes through the thick mask at a different angle. Thus, off-axis illumination with non-symmetric sources requires a modification of the left vs. right boundary layers, as analyzed in our previous work.[16] Quantifying the exact source dependence of the conclusions made here is left for future studies.

7. EXPERIMENTAL VERIFICATION WITH AIMS TOOL

We validate the influence of absorber height and sidewall angle on wafer phase using experiments on phase-shifting masks (ATT-PSM) with 90nm contact holes, each mask having a different absorber height and sidewall angle, which have been measured independently using Atomic Force Microscopy. These topographical parameters are compared with the phase recovered from the AIMS images in order to explore dependencies.

To recover the phase at the wafer, a stack of through-focus intensity measurements for each mask is captured in the Deep UV AIMS^{TM} tool, with quadrupole illumination but low sigma values (outer $\sigma < 0.5$). A modified

Downloaded From: http://proceedings.spiedigitallibrary.org/ on 11/08/2016 Terms of Use: http://spiedigitallibrary.org/ss/termsofuse.aspx

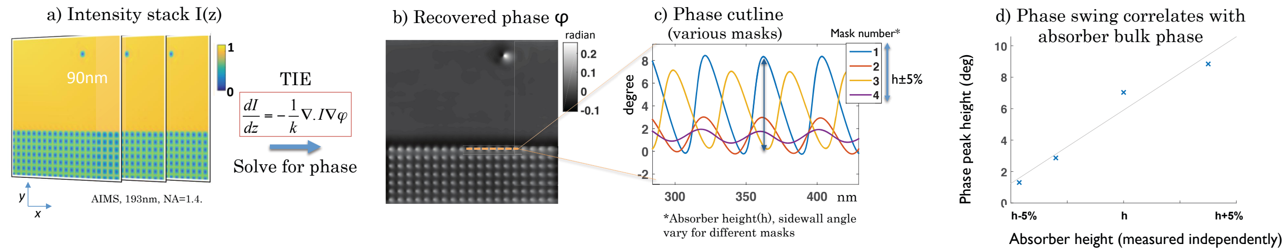

Figure 10. Validating dependence of measured phase swing on *bulk phase* for a set of phase-shifting masks with 90nm contact holes. a) Though-focus intensity images on an AIMS tool are used to calculate phase by solving the TIE. b) The recovered phase of the absorber at the wafer (modulo π). c) Cutlines of the recovered phase for various masks shows that the phase swings by different amounts for each case. d) The phase swing directly correlates with absorber height and hence *bulk phase* and no correlation is found with sidewall angle, confirming the dependences seen in simulation.

version of the TIE (Eq. 1) is solved in order to recover the phase at-focus from this dataset (Fig. 10b) using an iterative algorithm[17, 18] that has the added advantage of being robust to reasonable amounts of partial coherence.

Cutlines of the phase for each mask show a different peak phase swing in every case, despite the sidewall angle and absorber height (and hence *bulk phase*) varying between datasets. Simulations predict that the peak phase should increase only with the *bulk phase* (and hence absorber height), the *edge phase* being constant irrespective of absorber height. Furthermore, changes in the sidewall angle should not affect wafer-plane phase either. This in indeed confirmed by looking at the correlation of absorber height (and hence *bulk phase*) and peak phase swing in Fig. 10c. A good linear fit is seen across four different masks, confirming the trend predicted by simulation; no correlation is found with sidewall angle. Note that our experiments were done with phase-shifting masks, while studies in earlier sections used OMOG masks, confirming that the results hold for both mask types.

8. DISCUSSION

Thick mask diffraction effects influence intensity and phase at the wafer, impacting the process window. The two major contributors to unwanted phase at the wafer - *bulk phase* and *edge phase* - affect aerial imaging differently. While the *bulk phase* changes the phase swing at the aerial image, it does not affect phase gradients at the feature edge, so will not affect Bossung tilt. *Bulk phase* increases linearly with absorber height, but does not change with sidewall angle. The *edge phase* due to diffraction from mask sidewall, on the other hand, is independent of absorber height or sidewall angle fluctuations, but is responsible for the phase gradients at feature edges and hence is the main cause of tilting in the Bossung plots. In each case, an 8nm wide imaginary-valued thin mask boundary layer was found to approximate edge diffraction well, independent of feature size (at least down to the resolution limit).

It might be conjectured that the edge diffraction is insensitive to absorber thickness because the phase contribution from the edges is due to the break in the wavefront caused by the top and bottom corners of the absorber. Since the corners stay the same irrespective of absorber height, the edge diffraction would also be indifferent; the remaining change in sidewall length is already included in the *bulk phase* changes of the absorber.

The current study does have limitations. The topographical model used represents the absorber as a simple trapezoid with only two degrees of freedom, whereas actual thick mask profiles are more complex. Additionally, the effect of over-etch into the quartz, which would cause a two-level absorber stack (part quartz, part OMOG), has not been considered. Furthermore, the concept of *bulk phase*, i.e. phase due to a single pass through the absorber area, might need refining, since multiple reflections between the interfaces, which are ignored here, may cause multiple passes through the absorber before transmission.

Nevertheless, the broad principles found here could potentially be extrapolated to more sophisticated mask models, off-axis illumination and dense features. The sensitivity of the phase peaks at the wafer to absorber height at the mask opens up the potential for using phase imaging as a metrology method for investigating the phase of the absorber across a given mask, and for different masks. Another key finding is the constancy of edge diffraction (*edge phase*), which means that modeling edge effects in thick masks is as simple as adding phase corrections along the edges, which will be mostly independent of absorber topography fluctuations. This

Downloaded From: http://proceedings.spiedigitallibrary.org/ on 11/08/2016 Terms of Use: http://spiedigitallibrary.org/ss/termsofuse.aspx

is instructive for modeling thick mask effects on dense masks with tall absorber stacks (such as in EUV masks), where fast simulation models are needed despite large topography variations.

9. ACKNOWLEDGEMENTS

This work is sponsored by IMPACT+ (Integrated Modeling Process and Computation for Technology) member companies: Applied Materials, ARM, ASML, Global Foundries, IBM, Intel, KLA-Tencor, Mentor Graphics, Panoramic Tech, Qualcomm, Samsung, SanDisk and Tokyo Electron. AMTC is a joint venture of GLOBALFOUNDRIES and Toppan Photomasks.

REFERENCES

1. Faure, T., Gallagher, E., Hibbs, M., Kindt, L., Racette, K., Wistrom, R., Zweber, A., Wagner, A., Kikuchi, Y., Komizo, T., and Nemoto, S., "Characterization of binary and attenuated phase shift mask blanks for 32nm mask fabrication," *Proc. SPIE* **7122**, 712209–712209–12 (2008).
2. Bossung, J. W., "Projection printing characterization," in [*Developments in Semiconductor Microlithography II*], 80–85, International Society for Optics and Photonics (1977).
3. Shanker, A., Sczyrba, M., Connolly, B., Kalk, F., Neureuther, A., and Waller, L., "Critical assessment of the transport of intensity equation as a phase recovery technique in optical lithography," *Proc. SPIE* **9052**, 90521D–90521D–10 (2014).
4. Zibold, A. M., Scheruebl, T., Menck, A., Brunner, R., and Greif, J., "Aerial image measurement technique for today's and future 193-nm lithography mask requirements," *Proc. SPIE* **5504**, 12–18 (2004).
5. Teague, M. R., "Deterministic phase retrieval: a Green's function solution," *J. Opt. Soc. Am.* **73**(11) (1983).
6. Streibl, N., "Phase imaging by the transport equation of intensity," *Optics Communications* **49** (1984).
7. Adam, K. and Neureuther, A., "Simplified models for edge transitions in rigorous mask modelling," *Proc. of the SPIE* **4346**, 331–344 (2001).
8. Tirapu-Azpiroz, J., Burchard, P., and Yablonovitch, E., "Boundary layer model to account for thick mask effects in photolithography," *Proc. SPIE, Optical Microlithography XVI* **5040**, 1611–1619 (June 2003).
9. Miller, M., *Mask Edge Effects in Optical Lithography and Chip Level Modeling Methods*, PhD thesis, EECS Department, University of California, Berkeley (Dec 2010).
10. Finders, J., "The impact of mask 3D and resist 3D effects in optical lithography," *Proc. SPIE* **9052** (2014).
11. Burkhardt, M. and Raghunathan, A., "Best focus shift mechanism for thick masks," *Proc. SPIE* **9422** (2015).
12. Hibbs, M. S. and Brunner, T. A., "Phase calibration for Attenuating Phase-Shift Masks," *Proc. SPIE* **6152** (2006).
13. Shanker, A., Waller, L., and Neureuther, A. R., *Defocus based phase imaging for quantifying electromagnetic edge effects in photomasks*, Master's thesis, University of California, Berkeley (May 2014).
14. Pistor, T., "EM Suite FDTD," *http://www.panoramictech.com/* .
15. Erdmann, A., Evanschitzky, P., Neumann, J. T., and Gräupner, P., "Mask-induced best-focus-shifts in DUV and EUV lithography," *Proc. SPIE* **9426**, 94260H–94260H–11 (2015).
16. Shanker, A., Sczyrba, M., Lange, F., Connolly, B., Neureuther, A., and Waller, L., "Characterizing the dependence of thick-mask edge effects on illumination angle using AIMS images," *Proc. SPIE* **9426** (2015).
17. Volkov, V., Zhu, Y., and Graef, M. D., "A new symmetrized solution for phase retrieval using the transport of intensity equation," *Micron* **33**(5), 411 – 416 (2002).
18. Shanker, A., Tian, L., Sczyrba, M., Connolly, B., Neureuther, A., and Waller, L., "Transport of Intensity phase imaging in the presence of curl effects induced by strongly absorbing photomasks," *Appl. Opt.* **53**, J1–J6 (Dec 2014).

Downloaded From: http://proceedings.spiedigitallibrary.org/ on 11/08/2016 Terms of Use: http://spiedigitallibrary.org/ss/termsofuse.aspx